18. Berger MJ. *Improved point kernels for electron and beta ray dosimetry.* Washington DC: U.S. Department of Commerce, National Bureau of Standards; 1973:73–107.
19. Rhodes BA, Stern HS, Buchanan JA, Zolle I, Wagner HN. Lung scanning with 99mTc microspheres. *Radiology* 1971;99:613–621.
20. Weibel ER, ed. *Morphometry of the human lung.* New York: Academic Press; 1963:81–82.
21. De Labriolle-Vaylet C, Colas-Linhart N, Petiet A, Bok B. Morphological and functional status of leucocytes labeled with 99mTc-HMPAO. In: Sinzinger H, Thakur ML, eds. *Radiolabeled cellular blood elements.* New York: Wiley-Liss; 1990:119–129.
22. Tubiana M, Bertin M, eds. *Radiobiology radioprotection.* Paris, France; Presses Universitaires de France; 1989:43–44.
23. Kassis AI, Adelstein SJ. Does nonuniformity of dose have implications for radiation protection? *J Nucl Med* 1992;33:384–387.
24. Rodemann HP, Bamberg M. Cellular basis of radiation-induced fibrosis. *Radiother Oncol* 1995;35:83–90.
25. Watt DE, Khan S. *Cross-sections for the biological effectiveness of electrons in mammalians cells.* Lund, Sweden: Third International Symposium on Biophysical Aspects of Auger Processes; 1995:L13.

Simplifying the Dosimetry of Carbon-11-Labeled Radiopharmaceuticals

Mark C. Wrobel, James E. Carey, Phillip S. Sherman and Micheal R. Kilbourn

Division of Nuclear Medicine, Department of Internal Medicine, University of Michigan, Ann Arbor, Michigan

A two time-point sacrifice method is proposed as an alternative to conventional multiple time-point sacrifice methods to determine the organ cumulated activity of 11C-labeled radiopharmaceuticals. **Methods:** Rat biodistribution data for 10 11C-labeled radiopharmaceuticals were analyzed to determine organ cumulated activity. Data were obtained at four sacrifice intervals 2–5 min, 10–15 min, 30–45 min and 1–1.5 hr postinjection. The organ absorbed dose per unit administered radioactivity (mGy/MBq) was calculated using all four data points and combinations of limited data. The objective was to determine if a limited sampling technique would provide sufficient accuracy in estimating absorbed dose. **Results:** Residence times calculated using two time-points acquired during the first half-life of 11C were either equivalent or positively biased compared to using all sacrifice times. Overall, 87% of the residence times assessed were conservative compared to the multipoint method. For bladder organs, a consistent negative bias was observed with the reduced sacrifice method. **Conclusion:** Analysis of animal biodistributions using a reduced sacrifice protocol provides results in good agreement with and generally conservative to results using all sacrifice intervals. Correction factors are required for the urinary bladder and gallbladder when using the simplified technique due to bias. The bladder was often the limiting organ in determining human administered activity.

Key Words: dosimetry; PET; carbon-11

J Nucl Med 1997; 38:654–660

Human absorbed dose from 11C-labeled radiopharmaceuticals is initially estimated using animal tissue and organ biodistributions (1), typically in the rat. For a new 11C-labeled radiotracer, this determination will usually include measuring organ activities at four or five time-points during the first three or four physical half-lives of 11C, using four to six animals per time-point. Organ time-radioactivity profiles are obtained from the measured organ radioactivity and cumulated activity, residence time and organ absorbed dose per unit administered radioactivity are calculated (2,3).

Determination of animal radioactivity biodistributions for 11C-labeled radiotracers is not trivial. Difficulties include the short (20 min) physical half-life requiring a rapid sacrifice protocol and the use of a significant number of animals to provide high precision and accuracy in the determination. These issues have been recognized by Gatley (4), who recommended eliminating animal measurements and basing dose estimates on human cardiac output models. In addition, Schaumann et al. (5) recommended limiting the sacrifice data for long lived 14C-labeled agents. In contrast, we evaluated the use of a simplified technique which uses only two sacrifice intervals to assess residence time. Using animal biodistribution data for 10 11C-labeled radiopharmaceuticals, we compared dosimetry estimates with the simplified technique and showed that such an alteration yields acceptable estimates of the expected human dosimetry.

The accurate assessment of urinary bladder-wall dose and gallbladder-wall dose are often overlooked when evaluating new short-lived radiotracers. This is partly due to the difficulty of measuring the residence time for these organs as well as the perception that because of delayed filling and the short physical half-life of 11C, they will be of lesser dosimetric importance than organs that receive first-pass depositions from the blood pool. The urinary bladder contents and estimated gallbladder contents residence times in the rat for 10 11C radiotracers were estimated using measured organ activities and a set of conservative assumptions based on ICRP-53 recommendations (6). Results indicate that the bladder organs can be critical in determining the limiting dose of new 11C-labeled radiotracers for human patients.

THEORY

Given a single bolus injection of radioactivity, A_o, into the blood pool, the radioactivity in organ or tissue S can be estimated using the compartmental model:

$$\frac{A_s(t)}{A_o} = F_s \sum_{j=n+1}^{n+m} a_j \sum_{i=1}^{n} \left\{ a_i \frac{\lambda_j}{\lambda_j - \lambda_i} [\exp - (\lambda_i + \lambda_p)t - \exp - (\lambda_j + \lambda_p)t] \right\},$$

$$\text{Eq. 1}$$

where F_s is the fractional distribution to organ or tissue S; a_i is the fraction of F_s eliminated with biological removal constant λ_i; a_j is the fraction of F_s taken up with biological uptake constant λ_j; n is the number of elimination components; m is the number of uptake components; and λ_p is the physical decay constant (6).

For absorbed dose calculations in nuclear medicine, and, in particular, for short half-life tracers ($T_{1/2} \leq 20$ min), several simplifying assumptions to the above model may be applied. First, uptake is either based on a single component, or instantaneous uptake is assumed (6). Further, the effective removal of radioactivity from an organ is described by a single component, and short half-life radiotracers can be taken to be equal to the physical decay constant (6). With single uptake and excretion components, the above model becomes:

$$\frac{A_s(t)}{A_o} = F_s \times \frac{\lambda_j}{(\lambda_j - \lambda_i)} [\exp - (\lambda_i + \lambda_p)t - \exp - (\lambda_j + \lambda_p)t].$$

$$\text{Eq. 2}$$

TABLE 1
Carbon-11-Labeled Radiotracers Evaluated

| Abbreviation	Chemical name (behavior)
[^{11}C]EPI	[^{11}C]epinephrine (hydrophilic)
[^{11}C]mHED	[^{11}C]metahydroxyephedrine (hydrophilic)
[^{11}C]PHE	[^{11}C]phenylephrine (hydrophilic)
[^{11}C]MTBZ	[^{11}C]methoxytetrabenazine [lipophilic, amine)3°)]
[^{11}C]NMPB	[^{11}C]N-methyl piperidyl benzilate, lipophilic, amine (3°)]
[^{11}C]TBZ	[^{11}C]tetrabenazine [lipophilic, amine (3°)]
[^{11}C]TRB	[^{11}C](+)-2α-tropanyl benzilate [lipophilic, amine (3°)]
[^{11}C]FNZPAM	[^{11}C]flunitrazepam (lipophilic, amide)
[^{11}C]PK11195	[^{11}C]1-(2-chlorophenyl-N-methyl-N-(1-methylprophyl)-3-isoquinoline carboximide (lipophilic, amide)
[^{11}C]RAC	[^{11}C]raclopride (variable behavior)

The rat organ-time radioactivity profiles for the ^{11}C-labeled compounds listed in Table 1 show that the maximum organ radioactivity is found at the time of first sacrifice, which is either 2 or 5 min postinjection. Radioactivity then decreases according to either a mono-exponential or biexponential curve with inflection consistently occurring after the second sacrifice interval, 10 or 15 min postinjection. The trend in organ activity during the first 15 min postinjection indicates either initial drug washout with an effective removal constant ($\lambda_j + \lambda_p$) being greater than λ_p or delayed organ uptake with an effective removal constant less than λ_p but greater than zero. Sampling points after this period provide the tail of the biodistribution to four or five physical half-lives of the radiopharmaceutical. Exceptions to this finding are the urinary bladder and gastrointestinal tract which have complex profiles because of delayed filling and emptying. Removal of radioactivity in the tail region was observed to be mono-exponential and either predominantly or solely due to physical decay. These findings suggest that the above model may be revised to use two discrete time intervals. The first interval is characterized by single uptake and clearance components with physical decay and is identical to the original model. The second interval is characterized by a single clearance component weighted by physical decay (Fig. 1). A suitable compartmental model for first-compartment source organs, with a bolus injection of a ^{11}C radiotracer, then becomes:

$$A_s(t) = A_0 F_s \times \frac{\lambda_j}{(\lambda_j - \lambda_i)} [\exp - (\lambda_i + \lambda_p)t - \exp - (\lambda_j + \lambda_p)t]$$

$$t \leq 15 \text{ min}$$

$$A_s(t) = A_s(15)\exp - (\lambda_k + \lambda_p)t \quad t > 15 \text{ min.}$$

Eq. 3
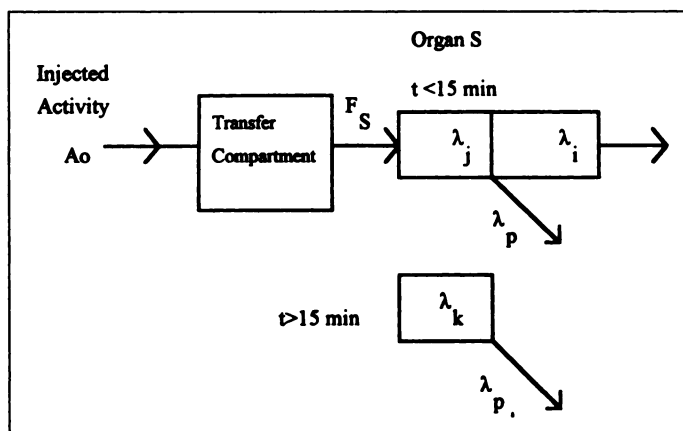
FIGURE 1. Simplified model proposed for ^{11}C-labeled radiopharmaceuticals. Removal of activity after the first half-life is assumed to be mono-exponential, with $\lambda_k \leq \lambda_p$.
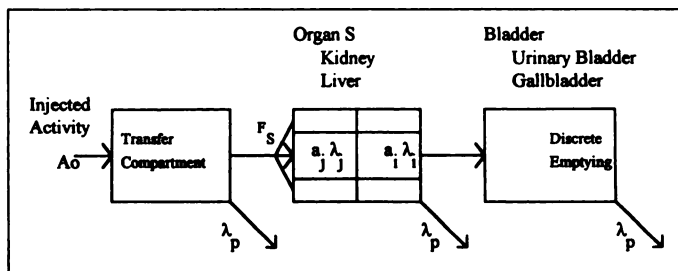
FIGURE 2. Three-compartment kinetics model for urinary bladder and gallbladder radioactivity determination. The model demonstrates a delayed uptake path to the bladder organ, which then empties in discrete time intervals. Since emptying times are long compared to the physical half-life of ^{11}C, biological removal is often ignored (6).

If this model is valid, and assuming λ_k is small, two sacrifice(d) intervals should then be sufficient to describe the biodistribution. This expected behavior allows us to present the hypothesis that differences will be small between biodistributions assessed from multiple sacrifice(d) data and that from a simplified method using two sacrifice(d) times, one very early postinjection and the second after one physical half-life of ^{11}C.

Urinary Bladder and Gallbladder

Simplified models have been developed to predict radioactivity in the urinary bladder (6–8) and gallbladder (6, 9–12) using two, three or more catenary compartmental models (Fig. 2). Such models, however, generally over-simplify the physiological processes involved and the complex relationship between urine or bile flow-rate, emptying periods and the volume present in the bladder that actually occurs (13,14). A three-compartmental model implies that sampling be performed at a minimum of six time-points, assuming that measured time-radioactivity profiles can be simplified to only three transfer coefficients. In practice, four to five time-points have been used to estimate bladder residence times, with data reflecting significant variability between animals at a given time of kill. Under such conditions, the simplifying assumptions made for solid first-pass organs are not valid for the bladder organs.

MATERIALS AND METHODS

To evaluate whether a reduced sacrifice(d) protocol is sufficient to estimate cumulated activity, the 10 ^{11}C-labeled radiotracers in Table 1 were examined. Biodistributions were evaluated at four sacrifice(d) times with four to five Sprague-Dawley rats (mixed sex) sacrificed per interval. Animals were injected intravenously (femoral vein) with up to 600 μCi of the subject radiotracer, prepared by the University of Michigan PET Facility. Subgroups were then sacrificed at intervals of 2–5, 10–15, 30–45 and 60–90 min postinjection and whole organs dissected out, weighed and assessed for ^{11}C in a sodium iodide well-counter. Source organs evaluated included: adrenals, brain, eyes, heart, kidneys, liver, lungs, ovaries, pancreas, small intestine, spleen, testes, urinary bladder contents and remainder of body. Remainder of body activity was measured with a dose calibrator. Organ cumulated activities and residence times were calculated from this data and a statistical analysis conducted to determine s.d. and confidence intervals. The results provided a reference for comparison with the proposed simplified technique. The reduced sacrifice method used the above data, but only one or two sacrifice intervals were used to characterize each radiotracer and organ. Cumulated activity and residence times assessed from the simplified method were compared using a Student's t-test and the percent difference from the conventional multiple point sacrifice method.

Five permutations of available data were tested. Three permutations used two sacrifice intervals: T1 and T2, T1 and T4 and T2

and T4, and two used a single sacrifice interval: either T1 or T2. Cumulated activities assessed from these simplified methods were compared using a Student's t-test and the percent difference from the multiple point sacrifice method.

The assessment of cumulated activity was determined using the method of Wagner et al. (15) modified for direct integration to determine the cumulated activity between each available data point. Because of the rapid uptake measured, activity before the first data point was obtained by assuming an exponential curve extrapolated back to the time of injection from the first two available data points. This resultant profile will be characterized by a y-intercept which gives a conservative value for the organ radioactivity at time equals zero and an effective removal constant equal to the slope of the curve. The method was also modified by assuming an exponential trend between data, in contrast to linear. For the specific case of ^{11}C compounds, where physical decay dominates the time-radioactivity profile, an exponential fit between sacrifice intervals is reasonable.

For the animal activities at each sacrifice interval, the sample average and sample s.d. were calculated. These were then used in the following expression to determine the cumulated activity in the organ from the time of injection to infinity:

$$\tilde{A}(0 \rightarrow \infty) = \frac{A_o}{\lambda_{eff(T_1 \rightarrow T_2)}} [1 - \exp(-\lambda_{eff(T_1 \rightarrow T_2)}T_2)]$$

$$+ (A_2 - A_3)\left(\frac{(T_3 - T_2)}{\ln(A_2) - \ln(A_3)}\right)$$

$$+ (A_3 - A_4)\left(\frac{(T_4 - T_3)}{\ln(A_3) - \ln(A_4)}\right)$$

$$+ 1.44 \times T_p \times A_4 . \qquad \text{Eq. 4}$$

The first term on the right of this expression determines the cumulated activity from the time of injection to the second sacrifice interval. The next two terms assess the cumulated activity between the second and third and then the third and fourth sacrifice intervals based on an integration between these points. The last term represents the cumulated activity from the final sacrifice interval to infinity with physical decay, the only removal mechanism. A_o and λ_{eff} are derived from the first two sacrifice activities and times, such that:

$$A_o = \exp\left(\frac{T_1 \times \ln(A_2) - T_2 \times \ln(A_1)}{T_1 - T_2}\right)$$

$$\qquad \text{Eq. 5}$$

$$\lambda_{eff}(T_1 \rightarrow T_2) = \left(\frac{\ln(A_2) - \ln(A_1)}{T_2 - T_1}\right).$$

For determination of the cumulated activity using a two or single sacrifice interval method, the expressions for cumulated activity reduce to:

$$\tilde{A}(0 \rightarrow \infty) = \frac{A_o}{\lambda_{eff(T_1 \rightarrow T_2)}} [1 - \exp(-\lambda_{eff(T_1 \rightarrow T_2)}T_2)]$$

$$+ 1.44 \times T_p \times A_2 \quad \text{(2 points)}$$

$$\tilde{A}(0 \rightarrow \infty) = 1.44 \times T_p \times [A_1 \exp(\lambda_p T_1) \quad \text{(1 point).} \qquad \text{Eq. 6}$$

Once the residence times in all source organs were established they were corrected using factors recommended by Roedler (16) to account for the difference in organ to total body-weight proportions between standard rat and standard human. Adult phantom S-values (mGy/MBq-s) for all important source-target pairs were obtained from the MIRDOSE III program (17), with the S-values for the rest of body assessed using the method of Coffey and Watson (18). The dose to a given target organ was then determined from the
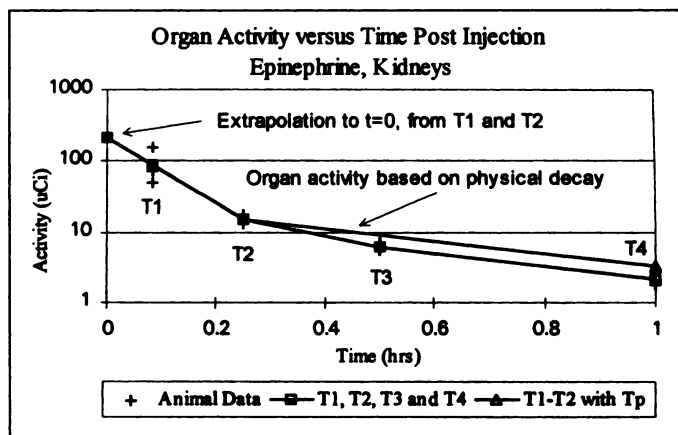

FIGURE 3. Biodistribution of [^{11}C]epinephrine in rat kidneys. Removal by physical decay only after the second sacrifice interval (top line).

conventional MIRD formula (19,20). Absorbed doses were determined for all source organs previously listed.

Dosimetry for Urinary Bladder and Gallbladder

Dosimetry for the urinary bladder and gallbladder required special consideration. Urinary bladder residence time was assessed in ligated male rats from the measured bladder contents. Female data were obtained from the radioactivity assessed as missing in the rat at the time of sacrifice. Missing radioactivity not accounted for in the measured organs and carcass was assumed to have been excreted by the animal during the waiting period between injection and sacrifice. The two measures were combined to calculate an effective cumulated activity, resulting in a conservative estimate of bladder residence time and subsequent absorbed dose per unit injected dose. For the purposes of this article, a conservative estimate of a parameter indicates a value larger than the true value.

The determination of a dose to the small intestine wall or gallbladder wall per unit injected radioactivity is impossible to assess in the rat since the animal has no gallbladder, and excretion from the liver is shunted directly to the small intestine. The ICRP indicates that for most very short-lived radiopharmaceuticals, gastrointestinal residence times can be ignored for dosimetric purposes (6), since clearance from the human gallbladder is considered to occur in bolus amounts, with the first clearance time at three hours postinjection which is long compared to the half-life of ^{11}C. It is assumed the radioactivity directly shunted to the small intestine results in a small overall dose to the intestine because of delayed uptake and its large mass and subsequently small S-value. A conservative determination of gallbladder wall dose was made using the ICRP-53 biliary excretion model which assumes that 30% of the biliary excretion would be deposited in the gallbladder (6). Thus, 30% of the measured small intestine residence time was used as an estimate for the gallbladder residence time.

RESULTS

This study included four to five animals per time point, with 13 animal organs evaluated at each time point for each of the 10 radiotracers. The most prevalent biodistribution observed (65% of cases) was characterized by a rapid maximum uptake at T1, followed by rapid clearance to the second sacrifice interval. After this time, removal was equal to or somewhat greater than that expected by physical decay. This biodistribution is demonstrated in Figure 3 and was most characteristic of the hydrophilic compounds such as [^{11}C]epinephrine and [^{11}C]m-HED. This behavior was also seen for [^{11}C]NMPB (lipophilic, amine), [^{11}C]FNZPAM (lipophilic, amide) and [^{11}C]raclopride,

TABLE 2
Residence Times and Absorbed Dose Per Unit Administered Activity for the Three Solid Organs Receiving the Largest Dose from Each Radiotracer

| Tracer | Source/target organ | Residence times (based on uncorrected rodent data) | | | Absorbed dose/unit administered activity (human estimates using Roedler factors) | | |
| | | All data | T1 and T2 only | | All data | T1 and T2 only | |
		$\tau_h \pm \sigma^*$ (s)	$\tau_h \pm \sigma^*$ (s)	%Diff[†]	$D/A_0 \pm \sigma^*$ (mGy/MBq) $\times 10^3$	$D/A_0 \pm \sigma^*$ (mGy/MBq) $\times 10^3$	%Diff[†]
EPI	Heart wall	32 ± 2.7	37 ± 5.0	−16%	16 ± 1.2	19 ± 2.4	−15%
	Kidney	88 ± 40	95 ± 36	−7.8%	12 ± 4.3	13 ± 4.5	−7.9%
	Liver	420 ± 39	440 ± 76	−4.8%	10 ± 0.91	11 ± 1.7	−5.2%
mHED	Heart wall	39 ± 3.3	41 ± 4.7	−4.8%	19 ± 1.8	21 ± 2.2	−4.9%
	Liver	370 ± 37	360 ± 49	0.35%	9.2 ± 0.67	9.2 ± 1.1	−0.19%
	Kidney	63 ± 48	69 ± 41	−11%	9.1 ± 4.7	10 ± 5.1	−9.8%
PHE	Ovaries	1.1 ± 0.19	1.1 ± 0.18	−3.2%	7.3 ± 0.72	7.1 ± 0.76	2.8%
	Kidney	41 ± 5.0	44 ± 5.8	−7.8%	6.3 ± 0.59	6.8 ± 0.73	−7.5%
	Heart wall	10 ± 0.74	12 ± 1.7	−17%	6.0 ± 0.50	7.0 ± 0.83	−16%
MTBZ	Ovaries	3.1 ± 0.53	2.9 ± 0.90	6.2%	15 ± 2.3	14 ± 3.8	4.8%
	Adrenals	3.5 ± 0.63	3.4 ± 1.1	1.0%	15 ± 2.5	15 ± 3.9	−0.25%
	Pancreas	32 ± 3.2	37 ± 6.6	−18%	8.9 ± 0.74	10 ± 1.5	−16%
NMPB	Ovaries	2.5 ± 0.39	3.3 ± 0.47	−29%	13 ± 1.7	16 ± 2.0	−22%
	Kidney	68 ± 13	72 ± 15	−6.6%	9.6 ± 1.7	10 ± 1.9	−6.6%
	Brain	74 ± 6.2	77 ± 7.4	−4.5%	9.5 ± 0.79	10 ± 0.93	−4.9%
TBZ	Adrenals	2.9 ± 0.48	3.3 ± 0.68	−16%	12 ± 1.8	14 ± 2.5	−14%
	Ovaries	2.1 ± 0.26	2.1 ± 0.15	−1.2%	11 ± 0.97	11 ± 0.65	−0.06%
	Pancreas	65 ± 5.8	62 ± 7.5	−16%	8.4 ± 0.88	9.5 ± 1.5	−13%
TRB	Lung	63 ± 6.2	75 ± 11	−17%	12 ± 1.1	14 ± 1.8	−16%
	Brain	80 ± 6.1	93 ± 12	−16%	10 ± 0.74	12 ± 1.6	−15%
	Heart wall	18 ± 1.0	23 ± 1.3	−24%	10 ± 0.60	13 ± 0.64	−21%
FNZPAM	Adrenals	1.5 ± 0.54	2.4 ± 0.91	−55%[‡]	7.0 ± 1.9	10 ± 3.3	−44%
	Liver	160 ± 27	210 ± 45	−28%	4.5 ± 0.54	5.6 ± 1.0	−23%
	Ovaries	0.34 ± 0.09	0.39 ± 0.08	−15%	4.1 ± 0.44	4.4 ± 0.42	−7.2%
PK11195	Adrenals	10 ± 2.3	9.5 ± 4.1	5.0%	39 ± 7.9	37 ± 15	4.2%
	Heart wall	72 ± 3.4	86 ± 3.7	−18%	36 ± 1.5	43 ± 1.8	−17%
	Ovaries	5.8 ± 1.8	6.7 ± 1.7	−15%	27 ± 6.7	31 ± 7.4	−13%
RAC	Ovaries	2.1 ± 0.47	2.3 ± 0.65	−8.9%	11 ± 2.1	12 ± 2.8	−7.5%
	Kidney	55 ± 8.2	67 ± 9.6	−20%	8.3 ± 0.96	9.7 ± 1.2	−17%
	Liver	230 ± 15	270 ± 21	−20%	6.3 ± 0.35	7.3 ± 49	−15%

*The s.d. of the residence time in seconds or the absorbed dose per unit administered radioactivity in mGY/MBq $\times 10^3$.

[†]The percent difference between the residence times or absorbed dose for the two methods, where a negative percent difference indicates a conservative (higher) result using the simplified technique.

[‡]Anomalous difference based on small organ activities and difficulty in precise determination of adrenal organ activity.

with the biodistribution exhibiting significant biological removal after the second sacrifice interval. Delayed organ uptakes were demonstrated for the liver and testes of all hydrophilic compounds and for most organ uptakes of [¹¹C]TBZ, [¹¹C]MTBZ and [¹¹C]TRB, accounting for 20% of the cases examined. The radioactivity measured in the carcass and remaining tissues typically followed a monoexponential profile of pure physical decay, accounting for 15% of the cases.

Because biodistributions varied dramatically during the first 15 min postinjection, the only acceptable reduced sacrifice permutation required use of the two sacrifice intervals measured within the first physical half-life of ¹¹C. This method had the advantage of preserving information during the period when biological uptake and clearance played a significant role determining the time-radioactivity profile. After the second time of sacrifice, physical decay was assumed to be the only removal mechanism. All other attempted permutations failed to adequately estimate the cumulated activity.

The rodent based residence times and estimated human organ absorbed doses were determined using all four sacrifice intervals

and only the first two sacrifice intervals are compared in Table 2 for the three solid organs receiving the highest dose per unit activity. The residence time assessed from the simplified method varied from being 50% larger (conservative) to 15% smaller than that assessed using the all available time points. In 64% of the cases, residence times were assessed as being 0%–20% higher using the simplified method. In 86% of the cases, a conservative measure of residence time resulted as compared to using all data. For those cases where a positive percent difference was measured (i.e., the cumulated activity assessed from all data were greater than that assessed using the reduced method), the difference was small, and typically there was no statistical difference between the values as indicated by a Student's t-test. In only 8% of the cases there was a statistically significant difference between methods, up to a maximum difference of 15%.

Similar results were observed in the determination of absorbed dose where the average percent difference between the reduced sacrifice technique and the multipoint technique was 8%. The range of differences between the two methods was from 55% larger (conservative) to 19% smaller. In over half the

TABLE 3
Residence Times and Absorbed Dose per Unit Administered Activity for the Urinary Bladder Wall and Gallbladder Wall

| Tracer | Source/target | Source residence times (All data T1 and T2 only) | | | Target absorbed dose/unit administered activity (All data T1 and T2 only) | | | |
		$\tau_h \pm \sigma$ (s)	$\tau_h \pm \sigma$ (s)	%Diff[†]	$D/A_0 \pm \sigma$ (mGy/MBq) × 10^3	$D/A_0 \pm \sigma$ (mGy/MBq) × 10^3	%Diff[†]	Method[‡]
EPI	UB/UB	240 ± 79	250 ± 20	−5.7%	46 ± 15	49 ± 3.7	−6.1%	1
	SI/GB	122 ± 24	110 ± 23	9.7%	26 ± 4.6	24 ± 4.5	7.6%	
mHED	UB/UB	260 ± 23	160 ± 51	39%	50 ± 4.4	31 ± 9.6	38%	2
	SI/GB	na	na		na	na		
PHE	UB/UB	450 ± 27	300 ± 26	33%	85 ± 5.0	58 ± 5.0	32%	3
	SI/GB	82 ± 18	73 ± 7.5	11%	18 ± 3.5	17 ± 1.5	8.6%	
MTBZ	UB/UB	18 ± 0.96	17 ± 0.37	3.7%	6.0 ± 0.20	6.0 ± 0.14	−0.82%	2
	SI/BG	95 ± 12	96 ± 17	−1.3%	21 ± 2.3	22 ± 3.3	−2.3%	
NMPB	UB/UB	390 ± 37	270 ± 73	32%	74 ± 6.9	51 ± 14	31%	4
	SI/GB	320 ± 29	267 ± 46	15%	63 ± 5.6	54 ± 8.9	14%	
TBZ	UB/UB	110 ± 25	71 ± 32	36%	23 ± 4.7	16 ± 5.9	32%	4
	SI/GB	66 ± 5.8	62 ± 7.2	5.1%	16 ± 1.1	15 ± 1.5	3.7%	
TRB	UB/UB	138 ± 30	87 ± 60	37%	28 ± 5.6	19 ± 11	34%	
	SI/GB	na	na		na	na		
FNZPAM	UB/UB	360 ± 58	400 ± 71	−9.7%	70 ± 11	76 ± 13	−9.3%	3
	SI/GB	na	na		na	na		
PK11195	UB/UB	330 ± 100	350 ± 178	−6.9%	64 ± 19	68 ± 33	−6.1%	1
	SI/GB	na	na		na	na		
RAC	UB/UB	na	na		na	na		
	SI/GB	160 ± 29	130 ± 50	20%	35 ± 5.5	28 ± 9.6	19%	

*The s.d. of the residence time in seconds or the absorbed dose per unit administered radioactivity in mGy/MBq × 10^3.

†The percent difference between the residence times or absorbed dose for the two methods, where a negative percent difference indicates a conservative (higher) result using the simplified technique.

‡Method by which animal urinary bladder radioactivity was determined: (1) men used measured bladder contents, women used unrecovered radioactivity; (2) bladder radioactivity based on male bladder contents, essentially 100% recovery in women; (3) urine not collected, bladder radioactivity estimated from missing radioactivity at time of sacrifice, women only; (4) urine not collected, bladder radioactivity estimated from missing radioactivity at time of sacrifice, men and women.

UB/UB = urinary bladder contents (source) and urinary bladder wall (target); SI/GB = small intestine contents (source) and gallbladder wall (target); na = not available.

cases, there was less than a 10% difference between the two methods, and in over 85% of the cases there was less than a 20% difference between the two methods. There was a positive percent difference measured in only 10% of the cases, and these differences were within the s.d. of the calculated organ doses.

Urinary Bladder and Gallbladder

Residence times for urinary bladder contents and estimated gallbladder contents, as well as the dosimetry for the gallbladder wall and urinary bladder wall are presented in Table 3. The s.d. in urinary bladder residence times was on the order of 5%–50% and were reasonable considering the expected variability between male bladder contents and the radioactivity assessed as missing from the female rats. The s.d. for the gallbladder contents ranged from 10%–20%. The bladder data indicated a consistent negative bias between the multiple time-point and reduced sacrifice methods for many of the radiotracers, on the order of 30%–40% (i.e., the reduced sacrifice method provided a smaller measure of residence time than the current method). This is largely attributable to the delayed filling of these organs which is not assessed when using a reduced number of sampling points. Similar results are observed for the estimated gallbladder residence time and gallbladder wall dose. A maximum negative bias of 20% was measured between the four time-point and two time-point methods, again indicative of the delayed uptake in the gallbladder from the liver-biliary pathway.

DISCUSSION

Application of a reduced sacrifice technique based on a two-compartmental model provides estimates of residence time and absorbed dose per unit injected activity in good agreement with using multipoint sacrifice methods. This proposed simplification in biodistribution assessment provides several advantages over that proposed by Gatley (4), which determined theoretical upper limits of dose based on cardiac output models. Use of only modeled biodistribution can be overly conservative and does not necessarily provide good agreement with the radiotracer's measured biodistribution. With animal data, conservatism is maintained, and actual organ activities are relied upon for dose estimation.

Two organs that demonstrated consistently large cumulated activities were the urinary bladder and estimated gallbladder contents, with high absorbed doses resulting for the urinary bladder and gallbladder wall, respectively. Comparing the absorbed dose data between the bladder and solid organs, it is apparent that the urinary bladder is frequently the critical organ limiting administered radioactivity. The exceptions include: [11C]raclopride for which the gallbladder is limiting and [11C]MTBZ where the ovaries are limiting. However, considerable difficulty was encountered in determining a time-radioactivity profile for these organs. For the case of the urinary bladder, only two or three male rats were currently used per time-point. Because the measured urine radioactivity can vary significantly between these animals due to physiological differ-

ences, a valid residence time was difficult to establish. The current method does not address any diluting volume of urine at the time of ligation, and the bladder may be so expanded from urine accumulation at the time of sacrifice that it may affect measured kidney radioactivity. Further, the ligation may fail or the animal can remove the ligation if not properly restrained causing a loss of data. Instead, urinary bladder residence time was conservatively assessed from a combination of the available male data and the radioactivity assessed as missing in female rats at the time of sacrifice. The conservatism introduced by using only missing data from the female is evident for [¹¹C]phenylephrine and [¹¹C]FNZPAM where bladder residence times are considerably larger than other radiotracers. Similar observations are made in assessing the residence time of the gallbladder contents, convoluted by the lack of a gallbladder in the rat. The additional complication of rat bladder dosimetry is its applicability to the human. The metabolic differences between rat and human contribute additional conservatism to the measured bladder wall doses (21).

Because of the variability in bladder organ time-radioactivity profiles, the described reduced sacrifice technique requires particular consideration when applied to estimating bladder residence times. Table 3 shows that correction of the measured urinary bladder residence time by 40% will result in good agreement between the two methods, with a range in bias from 0% to 50% (conservative). A similar correction of 20% can be applied to gallbladder residence times assessed with the two-point method to correct its negative bias, providing a range of differences from 0%–22% (conservative). If necessary, refinement of the estimated urinary bladder dose can be performed using metabolic cages and application of the dynamic bladder model (7). Unfortunately, the short half-life of ¹¹C prevents a similar method for in-vitro verification of the gallbladder wall dose. Alternatively, bladder data is perhaps best determined "after the fact" from actual human subjects based on in vivo quantification and in vitro measurement of samples. Since the urinary bladder was commonly the limiting organ in terms of allowable injectable dose, collection of actual human data is important to validate the conservative and error prone animal data.

Recent recommendations of the ICRP (22) have supported the use of effective dose in the determination of risk compared with benefit in biomedical research. The current tissue weighting factor for the gonads is four times that of the urinary bladder (23), placing greater significance in the gonadal dose in determining limiting patient dosage. Should present regulatory bodies adopt ICRP recommendations, increased emphasis will be placed in the accurate determination of both gonadal dose and bladder doses, since these organs were found to receive the maximum absorbed dose overall. Since both organs are assessed with limited precision in mixed sex animal studies, validation of these organ biodistributions in higher animals or during initial human trials will have increased importance.

CONCLUSION

Measurement of residence time can be performed conservatively and quickly using a reduced sacrifice method focusing on two intervals within one half-life postinjection. The method essentially reduces the time and animal sacrifice requirements by half, while still maintaining necessary accuracy. Considering the inaccuracies in using rat data to characterize human biodistributions, the use of this reduced sacrifice method provides results that are quite acceptable.

The measured biodistributions of both hydrophilic and lipophilic compounds indicates that the urinary bladder wall and gallbladder wall can be dosimetrically important. A correction

factor of 1.4 is required for urinary bladder residence times and 1.2 for estimated gallbladder residence time assessed using the reduced sacrifice technique due to the delayed filling of these organs. Regulations may limit organ doses from the experimental use of radiotracers to 30 mGy for the gonads, whole body and lens of eye and 50 mGy to other organs (24). Based on these limits, the most restrictive radiotracer activity that could be administered is 480 MBq (13 mCi) of [¹¹C]FNZPAM, where the bladder wall dose is limiting. All other radiotracers have considerably higher permissible activities. These activities should be sufficient for initial evaluation of a new radiotracer on current two-dimensional imaging systems. The advent of septaless three-dimensional imaging PET systems will provide significant improvements in sensitivity by as much as a factor of six to ten (25). This will subsequently allow researchers to investigate the performance of new radiotracers with doses well below the conservative dose limits assessed from the reduced sacrifice method. We recommend that investigators verify bladder time-radioactivity profiles in human subjects during initial imaging trials to refine the recognized conservative bladder measurements made in the rat.

REFERENCES

1. International Commission on Radiation Units, Measurements. *Methods of assessment of absorbed dose in clinical use of radionuclides.* ICRU Report 32. London: Pergamon Press; 1979.
2. Mullholland GK, Otto CA, Jewett DM, et al. Synthesis, rodent biodistribution, dosimetry, metabolism and monkey images of ¹¹C-labeled (+)-2α-tropanyl benzilate: a central muscarinic receptor imaging agent. *J Nucl Med* 1992;33:423–430.
3. Wong DF, Bice AN, Beck T, Dannals RF, Links JM, Wagner HN. Considerations for dosimetry calculations with neuroreceptor binding radioligands. *Fourth international radiopharmaceutical dosimetry symposium,* Oak Ridge Associated Universities, CONF-851113-(DE86010102); 1985:245–259.
4. Gatley JS. Estimation of upper limits on human radiation absorbed doses from ¹¹C-labeled compounds. *J Nucl Med* 1993;34:2208–2215.
5. Schaumann W, Neubert P. Animal experiments for estimating the radiation exposure of human subjects by radioactive drugs. *Pharmacology* 1988;37:333–340.
6. International Commission on Radiological Protection. *Radiation dose to patients from radiopharmaceuticals.* Oxford: Pergamon Press; ICRP Report; 1988:53.
7. Cloutier RJ, Smith SA, Watson EE, Snyder WS, Warner GG. Dose to the fetus from radionuclides in the bladder. *Health Physics* 1973;25:147–161.
8. Syed IB. Dosimetry of ¹¹³ᵐI radiopharmaceuticals with special attention to the urinary bladder. *Radiopharmaceutical dosimetry symposium.* HEW Publication (FDA 76–8044). Rockville, MD: Department of Health Education and Welfare, Bureau of Radiological Health; 1976:306–369.
9. MIRD, Medical Internal Radiation Dose Committee Estimate Report No. 7. Summary of current radiation dose estimates to humans from ¹²³I, ¹²⁴I, ¹²⁵I, ¹²⁶I, ¹³⁰I and ¹³¹I as sodium rose bengal. *J Nucl Med* 1975;16:1214–1217.
10. Koutoulidis C, Chiotellis E, Lymberis C. Absorbed dose estimation of some ⁹⁹ᵐTc-hepatobiliary agents. *Eur J Nucl Med* 1979;4:441–444.
11. Brown PH, Krishnamurthy GT, Bobby VR, Kingston E. Radiation-dose calculation for ⁹⁹ᵐTc-HIDA in health and disease. *J Nucl Med* 1981;22:177–183.
12. Brown PH, Krishnamurthy GT, Bobby VR, Kingston E, Turner FE. Radiation dose calculation for five ⁹⁹ᵐTc-IDA hepatobiliary agents. *J Nucl Med* 1982;23:1025–1030.
13. Snyder WS, Ford MR. Estimation of doses to the urinary bladder and to the gonads. *Radiopharmaceutical dosimetry symposium,* HEW Publication (FDA 76–8044). Rockville, MD: Department of Health, Education and Welfare, Bureau of Radiological Health; 1976:313–349.
14. Smith T, Veall, Wootton R. Bladder wall dose from administered radiopharmaceuticals: the effect of variation in urine flow rate, voiding interval and initial bladder content. *Radiat Prot Dosim* 1982;2:183–189.
15. Wagner HN, Smith EM, Brownell GL, Ellett WH. *Principles of nuclear medicine, radiation dosimetry.* Philadelphia: Saunders; 1968:742–784.
16. Roedler HD. Accuracy of internal dose calculations with special consideration of radiopharmaceuticals biokinetics. *Third international radiopharmaceutical dosimetry symposium.* Oak Ridge National Laboratory, HHS-Publication (FDA);1980:1–20.
17. Stabin MGMIRDOSE. Personal computer software for internal dose assessment in nuclear medicine. *J Nucl Med* 1996;37:538–546.
18. Coffey JL, Watson E. Calculating dose from remaining body activity: a comparison of two methods. *Med Phys* 1979;6:307–308.
19. Loevinger R, Berman M. *MIRD pamphlet no. 1, revised. A revised scheme for calculating absorbed dose from biologically distributed radionuclides.* New York: Society of Nuclear Medicine; 1976.

20. Berman M. *MIRD pamphlet no. 12: kinetics models for absorbed dose calculations.* New York: Society of Nuclear Medicine;1977.
21. McAfee JG, Subramanian G. Interpretation of interspecies differences in the biodistribution of radiative agents. *Third international radiopharmaceutical dosimetry symposium.* Oak Ridge National Laboratory, HHS-Publication (FDA); 1980:292–306.
22. International Commission on Radiological Protection. *Radiological protection in biomedical research.* Oxford: Pergamon Press; ICRP Report 62; 1993.
23. International Commission on Radiological Protection. Recommendation of the International Commission on Radiological Protection. Oxford: Pergamon Press; ICRP Report 1991;60.
24. Food and Drug Administration. Part 361: prescription drugs for human use generally recognized as safe and effective and not misbranded: drugs used in research. *Fed Reg* 1990;21:200–205.
25. Cherry SR, Dahlbom M, Hoffman EJ. Three-dimensional PET using a conventional multislice tomograph without septa. *J Comput Assist Tomogr* 1991;15:655–668.

Consequences of Using a Simplified Kinetic Model for Dynamic PET Data

Pamela G. Coxson, Ronald H. Huesman and Lisa Borland
Center for Functional Imaging, Lawrence Berkeley National Laboratory and Department of Physics, University of California, Berkeley, California

We compared a physiological model of ^{82}Rb kinetics in the myocardium with two reduced-order models to determine their usefulness in assessing physiological parameters from dynamic PET data. **Methods:** A three-compartment model of ^{82}Rb in the myocardium was used to simulate kinetic PET ROI data. Simulations were generated for eight different blood-flow rates reflecting the physiological range of interest. Two reduced-order models commonly used with myocardial PET studies were fit to the simulated data, and parameters of the reduced-order models were compared with the physiological parameters. Then all three models were fit to the simulated data with noise added. Monte Carlo simulations were used to evaluate and compare the diagnostic utility of the reduced-order models. A description length criterion was used to assess goodness of fit for each model. Finally, fits to simulated data were compared with fits to actual dynamic PET data. **Results:** Fits of the reduced-order models to the three-compartment model noise-free simulated data produced model misspecification artifacts, such as flow parameter bias and systematic variation with flow in estimates of nonflow parameters. Monte Carlo simulations showed some of the parameter estimates for the two-compartment model to be highly variable at PET noise levels. Fits to actual PET data showed similar variability. One-compartment model estimates of the flow parameter at high and low flow were separated by several s.d.s for both the simulated and the real data. With the two-compartment model, the separation was about one s.d., making it difficult to differentiate a high and a low flow in a single experiment. Fixing nonflow parameters reduced flow parameter variability in the two-compartment model and did not significantly affect variability in the one-compartment model. Goodness of fit indicated that, at realistic noise levels, both reduced-order models fit the simulated data at least as well as the three-compartment model that generated the data. **Conclusion:** The one-compartment reduced-order model of ^{82}Rb dynamic PET data can be used effectively to compare myocardial blood-flow rates at rest and stress levels. The two-compartment model can differentiate flow only if a priori values are used for nonflow parameters.

Key Words: PET; physiological models; rubidium-82; myocardial blood flow

Compartmental models represented by systems of linear differential equations are used to describe the time evolution of kinetic ROI data from PET (*1*). A three-compartment model of the disposition of ^{82}Rb in the myocardium is shown in Figure 1a, and the corresponding system of differential equations is:

$$\dot{x}_1(t) = -\left(\frac{F}{V_1} + \frac{PS_{cap}}{V_1}\right)x_1(t) + \frac{PS_{cap}}{V_2}x_2(t) + Fu(t), \qquad \text{Eq. 1}$$

$$\dot{x}_2(t) = \frac{PS_{cap}}{V_1}x_1(t) - \left(\frac{PS_{cap}}{V_2} + \frac{PS_{cell}}{V_2}\right)x_2(t) + \frac{PS_{cell}}{V_3^*}x_3(t), \qquad \text{Eq. 2}$$

$$\dot{x}_3(t) = \frac{PS_{cell}}{V_2}x_2(t) - \frac{PS_{cell}}{V_3^*}x_3(t), \qquad \text{Eq. 3}$$

where $\chi_i(t)$ denotes the time derivative of $\chi_i(t)$, which is activity in compartment i per volume of tissue.

The compartments are identified with physiological spaces—capillary, interstitial space and intracellular space. The input function u(t) consists of blood pool concentration of ^{82}Rb (activity per volume of blood). The transfer rates between compartments are expressed in terms of specific volume blood flow (F), permeability surface products (PS) for two physiological barriers, fractional volumes (V_i) of the interstitial and capillary spaces and the apparent volume of distribution factor (V_3^*) of ^{82}Rb in the intracellular space. Thus, we refer to this model as a physiological compartmental model. More complex models incorporating features such as heterogeneous flow rates, variable capillary length and axial diffusion have been used to fit multiple tracer dilution data (*2–4*). However, we will be making comparisons with smaller models and will refer to this three-compartment model as *the* physiological model and to its parameters as *the* physiological parameters.

PET data consist of estimated total emissions from an ROI. Regions have linear dimensions on the order of millimeters, which are too large to provide separate data for capillary, interstitial and intracellular compartments. Emission counts estimated from tomographic line integrals are affected by numerous sources of error reflecting both physical limitations (*5–8*) and methodological factors (*9–11*). Because of the coarseness of the measurements and the cumulative effect of errors in the measurements, it is not feasible to estimate all of the parameters of Figure 1a from the PET data alone.

For this reason, PET kinetic analysis has typically been performed with lower order compartmental models. The two- and one-compartment models shown in Figures 1b and c are among those that have been employed (*12–14*). The parameter of interest in most PET kinetic studies of the myocardium is specific volume flow (per min), and models are judged on their ability to distinguish between rest-flow rates around 1 per min and stress-flow rates of 3 or 4 per min.

For all models considered here, the PET measured data y(t)